The $P2X_7$ receptor from *Xenopus laevis*: formation of a large pore in *Xenopus* oocytes

Martin Paukert, Susanti Hidayat, Stefan Gründer*

Department of Otolaryngology, Research Group of Sensory Physiology, Röntgenweg 11, D-72076 Tübingen, Germany

Received 2 January 2002; accepted 9 January 2002

First published online 31 January 2002

Edited by Maurice Montal

Abstract The purinergic $P2X_7$ receptor is an ATP-receptor channel predominantly expressed in immune cells. $P2X_7$ has been cloned from human, rat and mouse. Here we report cloning of the *Xenopus laevis* $P2X_7$ receptor ($xP2X_7$). $xP2X_7$ is only about 50% identical to the mammalian homologues, shows a broad tissue expression pattern, and has the electrophysiological characteristics typical of a $P2X_7$ receptor: low agonist affinity (EC_{50} about 2.6 mM) and a non-desensitizing current. Moreover, expression of $xP2X_7$ in *Xenopus* oocytes is sufficient to induce the formation of a large pore, which is permeable to large cations such as $NMDG^+$. Identification of a non-mammalian $P2X_7$ receptor may help to identify functionally important parts of the protein. **© 2002 Federation of European Biochemical Societies. Published by Elsevier Science B.V. All rights reserved.**

Key words: P2 purinoceptor; Ion channel; Two-electrode voltage-clamp; Ion selectivity

1. Introduction

P2X receptors are ion channels gated by extracellular ATP. So far, seven different P2X subunits have been cloned ($P2X_{1-7}$), which form a gene family [1]. They have two transmembrane domains with intracellular termini and a rather large extracellular loop [2,3] and form non-selective cation channels with a high permeability to Ca^{2+}. Various P2X receptors show differences both in the affinity to ATP and in the kinetics of activation and inactivation. $P2X_1$ and $P2X_3$ show high agonist affinity (EC_{50}, ~1 μM) and rapid activation and desensitization, whereas $P2X_2$, and $P2X_{4-6}$ have a low agonist affinity (EC_{50}, ~10 μM), are slowly activating, and show only partial desensitization. $P2X_7$ shows the lowest agonist affinity (EC_{50}, 100–1000 μM), slow activation, and almost no desensitization [4–6]. Moreover, it is believed that the free ATP ion, ATP^{4-}, is the effective agonist at $P2X_7$, since solutions lacking Mg^{2+} and Ca^{2+} give greater agonist potency. And, ATP is only a partial agonist, since the ATP analogue 3′-*O*-(4-benzoyl)-benzoyl-ATP (BzATP) has an approximately 10-fold lower EC_{50} [4–6].

*Corresponding author. Fax: (49)-7071-22917.
E-mail address: stefan.gruender@uni-tuebingen.de (S. Gründer).

Abbreviations: cDNA, complementary DNA; cRNA, complementary RNA; BzATP, 3′-*O*-(4-benzoyl)-benzoyl-ATP; HMA, *N*,*N*-hexamethylene amiloride; KN-62, 1-[*N*,*O*-bis(5-isoquinolinesulfonyl)-*N*-methyl-L-tyrosyl]-4-phenylpiperazine; NMDG, *N*-methyl-D-glucamine

These properties of the $P2X_7$ receptor match the properties of the P2Z receptor, which had been characterized on immune cells, especially macrophages [7–11]. Another characteristic feature of the P2Z receptor is the fact that prolonged activation or repeated activation of the channel leads to the appearance of a large, unselective pore, which is permeable to organic cations of a size up to 900 Da. Expression of the $P2X_7$ receptor in various heterologous expression systems reconstitutes this property leading to the formation of a large pore and eventually to cell lysis [4–6]. There are, though, conflicting reports on the formation of the large pore in *Xenopus* oocytes, a commonly used expression system. It has been reported that expression of the rat $P2X_7$ receptor leads to formation of the large pore [12] as well as that neither expression of the rat nor of the human $P2X_7$ receptor are sufficient for formation of the large pore in *Xenopus* oocytes [13,14]. This has been taken as evidence that factors other than the $P2X_7$ receptor are necessary for ATP-induced permeabilization. Since the P2Z receptor has cytolytic properties in macrophages and since this property may have important functions in the immune system, understanding of the mechanism that governs formation of the large pore is a prerequisite for a deeper understanding of the function of the $P2X_7$/P2Z receptor in the immune system.

Here we report cloning of the *Xenopus* $P2X_7$ receptor. Expression of this new orthologue leads to formation of a typical $P2X_7$ phenotype characterized by low agonist affinity and incomplete desensitization. Moreover, prolonged agonist application leads to the formation of a large pore permeable to cations such as *N*-methyl-D-glucamine $(NMDG)^+$ (195 Da) in *Xenopus* oocytes. Cloning of the amphibian $P2X_7$ receptor may facilitate our understanding of the large pore formation and identification of functionally important parts of the protein.

2. Materials and methods

2.1. Cloning of $xP2X_7$

An expressed sequence tag (EST) from *Xenopus laevis* (accession number: BE509086; IMAGE clone ID: 3397314; provided by the Resource Center/Primary Database, Berlin, Germany) showing homology to $P2X_7$ receptors was entirely sequenced. It contained the 3′-end of the coding sequence and a long (2203 bp) 3′-untranslated region (3′-UTR). This sequence was used to design primers for rapid amplification of 5′-complementary DNA (cDNA) ends (5′-RACE), $xP2X_7$-5′RACE 5′-CCAATCGTCGGAAACCGTAATGAGG-3′ and, for the nested PCR reaction, $xP2X_7$-5′NRACE 5′-CAGTCCCAGTTGATCTCAATGCCC-3′. Using the SMART RACE cDNA amplification kit (Clontech, Palo Alto, CA, USA), 5′-RACE was performed with $polyA^+$ RNA from stomach of an adult *X. laevis* female.

0014-5793/02/$22.00 © 2002 Federation of European Biochemical Societies. Published by Elsevier Science B.V. All rights reserved.
PII: S0014-5793(02)02324-4

PCR products were subcloned using the TOPO-TA cloning kit (Invitrogen, Groningen, The Netherlands) and sequenced. One clone of about 1300 bp contained the entire 5′-coding region and 530 bp of 5′-UTR. The 5′-UTR contained an in-frame stop codon upstream of the methionine.

For expression studies, the entire coding sequence of $xP2X_7$ was amplified from *Xenopus* stomach cDNA by PCR using Expand High Fidelity (Roche, Mannheim, Germany). PCR primers were $xP2X_7$-5′ 5′-CCGGAGCTCGCCCTGCAGAAATGACACTGACC-3′ and $xP2X_7$-3′ 5′-CGGGGTACCTTATGGGCCTTCTGTTTG-CAGG-3′. Using terminal restriction endonuclease recognition sequences (*Sac*I and *Kpn*I), the PCR product was ligated in the oocyte expression vector pRSSP containing the 5′-UTR from *Xenopus* β globin and a poly(A) tail. Several clones from two independent PCR reactions were sequenced to exclude PCR errors.

The full-length sequence of $xP2X_7$ (accession number: AJ345114) was assembled from the 5′-UTR of the RACE product, the coding sequence of the expression construct and the 3′-UTR from EST clone BE509086.

A second EST obtained from *X. laevis* cDNA (accession number: BG814668; IMAGE clone ID: 4173287; provided by the RC/PD) was sequenced. This clone contained the entire coding region of $xP2X_7$, which was interrupted by an intron of 234 bp. The sequence of this EST showed the following amino acid exchanges compared to $xP2X_7$ cloned by PCR: F41Y, N105K, A224T, I238M, T267K, Q314K, Y364N, H376N, and E472Q. There were six additional nucleotide differences not changing the amino acid.

2.2. Semiquantitative RT-PCR

Total RNA was isolated from *Xenopus* tissues with peqGOLD RNApure (peqLab). It was digested with DNase, integrity of RNA checked on an agarose gel and 2 μg reverse transcribed using oligo-dT and SuperScript (Life Technologies, Karlsruhe, Germany). 1/13 of the reaction was amplified for 30 cycles (94°C for 30 s, 66°C for 30 s, 72°C for 5 s). PCR primers were $xP2X_7$-RT-u 5′-TATGCTGCCTC-CTGCCTGG-3′ and $xP2X_7$-RT-l 5′-CAGCAGTTGGGGATCACT-GC-3′. Amplification products were transferred to nylon membrane and then probed with a ^{32}P-labeled 500-bp *Bgl*II cDNA fragment from $xP2X_7$. Primers for control amplification of GAPDH were xGAPDH-RT-u 5′-TCACAACCACAGAGAAGGCC-3′ and xGAP-DH-RT-l 5′-CCATCTCTCCACAGCTTGCC-3′. Amplification was for 30 cycles (94°C for 30 s, 60°C for 30 s, 72°C for 10 s).

2.3. Electrophysiology

Oocytes, which had been surgically removed from female *X. laevis*, were injected with 30–100 pg of cRNA encoding $xP2X_7$. They were incubated at 19°C in OR-2 solution containing (in mM) NaCl 82.5, KCl 2.5, Na_2HPO_4 1.0, HEPES 5.0, polyvinylpyrrolidon 0.5 g/l, $MgCl_2$ 1.0, $CaCl_2$ 1.0 (pH 7.3). On the following day, the oocytes were treated with collagenase type II (0.33 g/l; Sigma-Aldrich, Deisenhofen, Germany) for 40 min in order to facilitate the removal of the follicular membrane, which was done a further day later.

Measurements were done at room temperature 3–7 days after injection using two-electrode voltage-clamp. Currents were recorded and filtered at 100 Hz with a TurboTec 03X amplifier (npi electronic GmbH, Tamm, Germany), digitized at 1 kHz using the AD/DA interface PCI 1200 (National Instruments, Austin, TX, USA) and stored on hard disk. Complete solution exchange at whole oocytes could be obtained within less than 1 s [15] using the oocyte testing carousel controlled by the interface OTC-20 (npi electronic GmbH). Data acquisition and solution exchange were managed using the software CellWorks 5.1.1 (npi electronic GmbH). The bath solution had the following composition (in mM): NaCl or NMDGCl 98.0, HEPES 5.0, niflumic acid 0.1 (pH 7.45). Niflumic acid was used to block the large conductance induced in oocytes by divalent-free extracellular solutions [16]. Divalent-free extracellular solutions were used in order to permit formation of a large unselective pore by $P2X_7$ receptors. ATP, *N*,*N*-hexamethylene amiloride (HMA), BzATP, collagenase, 1-[*N*,*O*-bis(5-isoquinolinesulfonyl)-*N*-methyl-L-tyrosyl]-4-phenylpiperazine (KN-62) and niflumic acid were all purchased from Sigma-Aldrich, Deisenhofen, Germany.

2.4. Data analysis

Current amplitudes for concentration–response curves were estimated using the calculated maximum value of a fit to the exponential rise phase of the current trace (Igor PRO, WaveMetrics, Lake Oswego, OR, USA). In order to minimize induction of large pore formation in experiments for concentration–response curves a two-pulse protocol was used: the first current pulse (4 s) was induced by the reference concentration of agonist (1 mM ATP/100 μM BzATP), the second one was induced by the testing concentration of agonist. Current amplitudes induced by testing concentrations were then normalized to the amplitudes induced by the reference concentration. The two-pulse protocol was also carried out with the reference concentration as testing concentration to estimate reproducibility of channel activation. The resulting concentration–response curves were fitted using the logistic function: $A+(B-A)/[1+(EC_{50}/C)^D]$, where A is the minimum response, B is the maximum response, C is the concentration, EC_{50} is the concentration at which half-maximal response is obtained, and D is the Hill coefficient. For better comparison of concentration–response curves with ATP and BzATP, values were then normalized to the maximum response B obtained from the respective fit.

Voltage ramps, which were used to determine reversal potentials, were run from −120 mV to +20 mV within 1 s. Current traces were leak-subtracted (Igor Pro). The shift in reversal potential in experiments using extracellular solution with $NMDG^+$ compared to experiments using extracellular solution with Na^+ were used to calculate relative permeabilities: $P_{NMDG}+/P_{Na}+ = \exp(\delta E_{rev}F/RT)$, where $P_{NMDG}+$ is the permeability to $NMDG^+$, $P_{Na}+$ is the permeability to Na^+ and δE_{rev} is the shift in reversal potential. F, R and T have their usual meanings. Results are reported as mean ± S.D. Statistical analysis was done with Student's t-test.

For YO-PRO-1 experiments, each oocyte was injected with 10 ng of cRNA encoding $xP2X_7$. YO-PRO-1 was purchased from Molecular Probes (Eugene, OR, USA). Images were obtained using an Olympus AX-70 light microscope (Olympus Optical Corp., Hamburg, Germany) equipped with epifluorescence and stored using a digital camera and analySIS software (Soft Imaging System GmbH, Münster, Germany).

3. Results and discussion

3.1. Molecular cloning of X. laevis $P2X_7$

An EST was used to clone full-length $P2X_7$ from *X. laevis* (see Section 2). The cDNA for $xP2X_7$ codes for a protein of 553 amino acids (Fig. 1). It has all the hallmarks of P2X receptors: two hydrophobic domains, conserved cysteines between the hydrophobic domains, and a short N-terminus. The C-terminus of $xP2X_7$ is long (about 215 amino acids), which is a characteristic feature of $P2X_7$ receptors [4]. Overall homology to mammalian $P2X_7$ receptors is rather low (about 50% identity) as can be expected since species divergence between mammals and amphibians occurred over 300 million years ago. Sequence identity is significantly higher in the hydrophobic domains and in the putative extracellular loop between the hydrophobic domains.

Assuming that N- and C-termini are intracellularly located, $xP2X_7$ has six potential *N*-glycosylation sites (Fig. 1). The last four of these sites are conserved in rat, mouse and human $P2X_7$, whereas the first two are specific for $xP2X_7$. There are two neighboring consensus sites for phosphorylation by protein kinase C at the N-terminus and one at the C-terminus. One of the sites at the N-terminus is completely conserved in P2X receptors, whereas the other two sites are specific for $xP2X_7$. There are 10 cysteine residues in the putative extracellular loop of $xP2X_7$, which are conserved in all P2X receptors. At the cytoplasmic tail there are several conserved cysteine repeats, which may serve as additional membrane anchors via palmitoylation.

After cloning of $xP2X_7$, another EST clone showing homology to $P2X_7$ receptors became available in the database. This clone contains the entire coding region of $xP2X_7$, which is

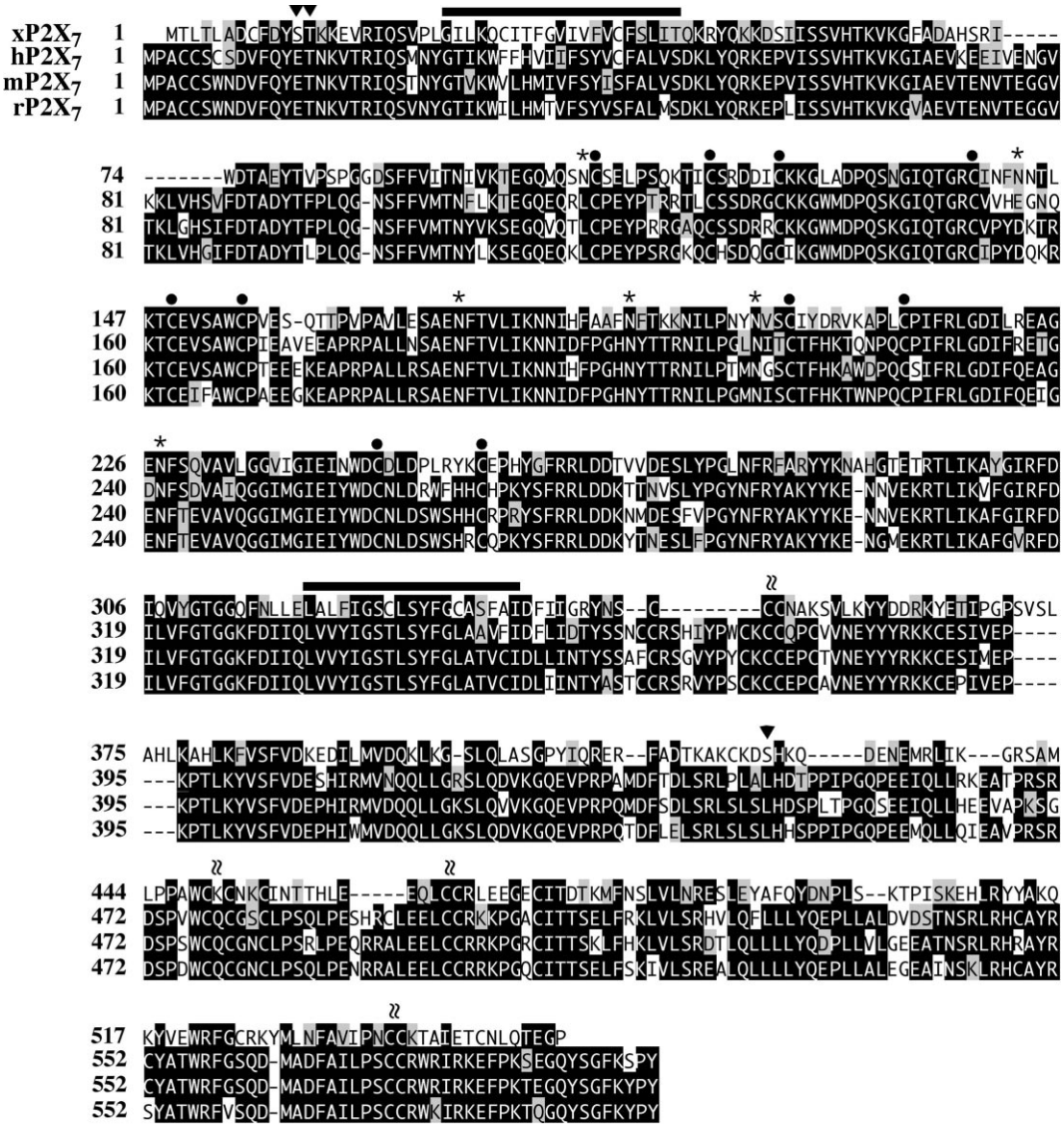

Fig. 1. Sequence alignment of $xP2X_7$ with its mammalian homologues. Amino acids showing a high degree of identity are shown as white letters on black background, those showing a high degree of homology as black letters on gray background. Transmembrane domains are indicated by bars, conserved cysteines by closed circles, potential glycosylation sites by asterisks, potential sites for phosphorylation by protein kinase C by arrowheads, and potential palmitoylation sites by wavy lines. Transmembrane domains have been predicted using the TMpred program (http://www.ch.embnet.org/). Accession number for $xP2X_7$ is AJ345114. Accession numbers for $hP2X_7$, $mP2X_7$, and $rP2X_7$ are Y09561, AJ009823, and X95882, respectively.

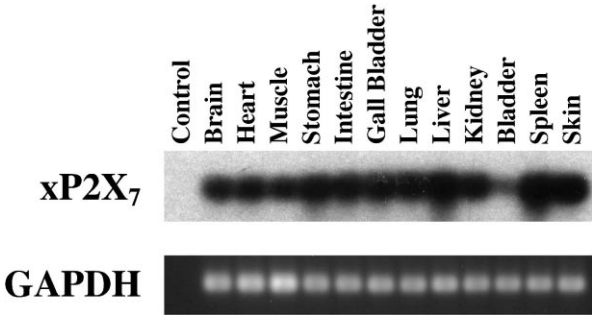

Fig. 2. RT-PCR analysis revealing broad tissue expression of $xP2X_7$ mRNA. PCR for GAPDH shows comparable amplification in all tissues examined. Control was without cDNA.

interrupted at the position corresponding to amino acid 234 by an intron of 234 bp. This intron contains several stop codons, which would lead to a premature end of the protein before the second transmembrane domain. Therefore, this clone most likely represents an immature transcript. When we amplified the coding sequence of $xP2X_7$, we found that a significant proportion ($>70\%$) of PCR products contained this intron. If a truncated $P2X_7$ receptor has a regulatory role remains to be investigated. Moreover, there are several amino acid differences between $xP2X_7$ and the EST clone (see Section 2). This may be due to strain variations or to polyploidy of *Xenopus*.

3.2. Analysis of $xP2X_7$ mRNA distribution

The expression of $xP2X_7$ was studied on a panel of different *Xenopus* tissues by RT-PCR. All 12 tissues tested were pos-

itive for xP2X$_7$ mRNA expression (Fig. 2). Abundance in bladder was low, whereas it was slightly higher in spleen, liver, skin, and stomach compared to other tissues. The P2X$_7$ receptor shows such a broad tissue expression pattern also in mammals [5]. mRNA expression in some of these tissues is probably due to infiltration by immune cells, but P2X$_7$ has recently also been detected in a variety of non-immune cells [17]. Given the high expression level of xP2X$_7$ in spleen, it is likely that immune cells express a P2X$_7$/P2Z receptor also in *Xenopus*. The immune system of amphibians shares all the basic cell types with the immune system of mammals and it is, therefore, likely that P2X$_7$ serves the same functions in the amphibian and in the mammalian immune system.

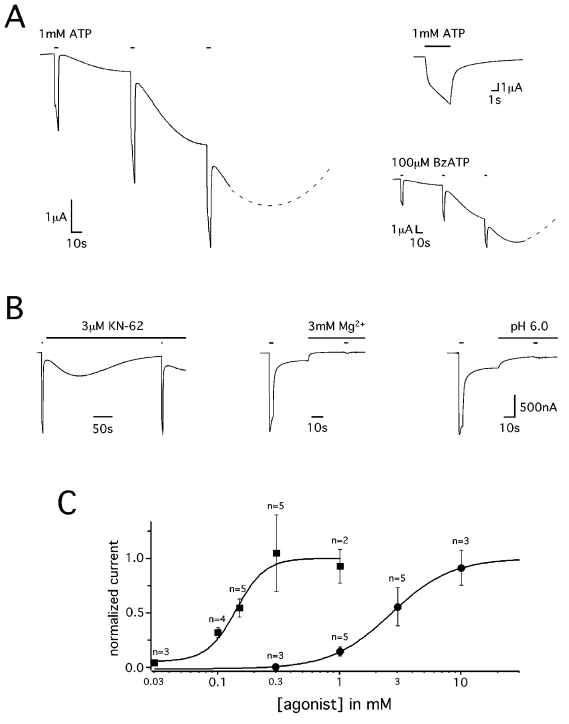

Fig. 3. Electrophysiological characteristics of xP2X$_7$. A: Left, representative current trace showing inward currents evoked by repetitive applications of ATP. A slowly increasing inward current appeared several seconds after washout of the agonist. Short ATP applications (1 mM for 4 s) were separated by washout for 60 s. Horizontal bars indicate agonist application. Holding potential was −60 mV. Upper right, enlargement of a representative current trace showing the kinetics of currents through xP2X$_7$. In some cases the current desensitized partially in the presence of agonist. Lower right, activation of xP2X$_7$ by the agonist BzATP elicited the same behavior as activation by ATP. B: Pharmacology of xP2X$_7$. Left, xP2X$_7$ was activated by ATP (1 mM ATP), then ATP was washed out and oocytes were incubated in KN-62 (3 μM) for 5 min followed by the second ATP pulse in the presence of KN-62. KN-62 did not significantly influence current amplitude. Also, the slowly activating current between ATP pulses was similar to control measurements ($n = 5$; $P > 0.05$). Middle, Mg^{2+} ions at a concentration of 3 mM blocked the fast activating as well as the slowly activating current (representative current trace). Right, extracellular protons at pH 6.0 also blocked both current components completely (representative current trace). C: Concentration–response curves for ATP (filled circle) and BzATP (filled square). Number of individual measurements for the corresponding testing concentration is indicated as *n*. Symbols represent mean ± S.D. EC_{50} was 2.6 mM and 139 μM for ATP and BzATP, respectively.

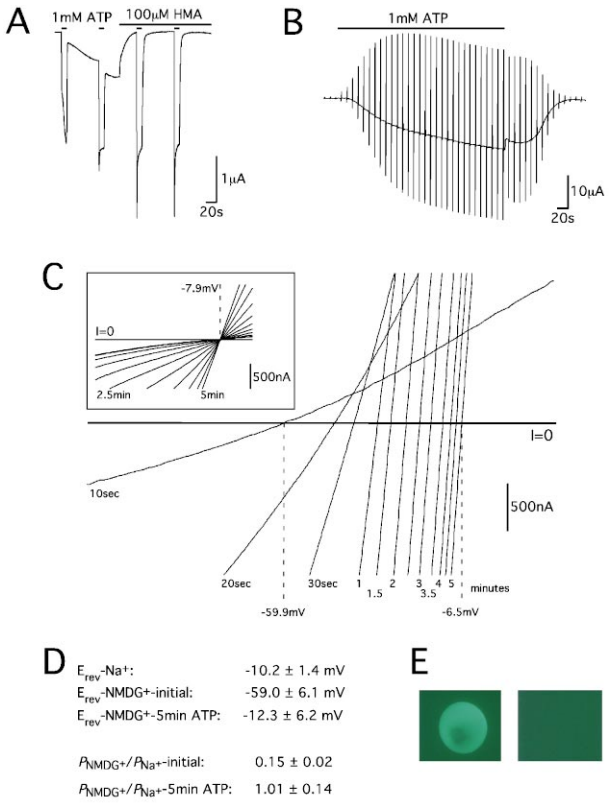

Fig. 4. Characterization of large pore formation by xP2X$_7$ in *Xenopus* oocytes. A: HMA (100 μM) blocked selectively and completely the slowly activating current, which appeared after washout of agonist ($n = 4$). The protocol used was as described for Fig. 3A. B: Membrane potential was clamped to −60 mV and every 10 s a voltage ramp (1 s) from −120 mV to +20 mV was run. Measurements were done in extracellular solution containing $NMDG^+$. ATP (1 mM) was applied continuously for 5 min. During ATP application a slowly increasing inward current appeared, which, upon washout, deactivated rapidly but partially. The remaining inward current showed a delayed deactivation. C: Current traces during voltage ramps at the indicated times after onset of agonist application from experiments shown in (B) are overlayed. The horizontal line indicates the level of zero current. During activation of xP2X$_7$ the reversal potential shifted significantly ($P < 0.001$) within 5 min, whereas it did not shift in measurements using the same protocol but with extracellular solution containing Na^+ (inset) ($n = 8$, each). D: Mean ± S.D. for reversal potentials (E_{rev}) and relative permeabilities ($P_{NMDG}+/P_{Na}+$). Increase of the relative permeability was around seven-fold. 'initial' is the value 10 s after onset of ATP application. E: Left, xP2X$_7$ expressing oocyte incubated in 10 μM YO-PRO-1 and 300 μM BzATP for 5 min. Fluorescence indicates dye uptake (not quantified). A similar picture was seen in six out of six experiments. Right, as a control, non-injected oocytes were analyzed using the same protocol. No dye uptake was seen in six out of six experiments.

3.3. Functional expression of xP2X$_7$ in Xenopus oocytes

Brief application of 1 mM ATP for 4 s to oocytes expressing xP2X$_7$ receptors evoked an inward current, which consisted of an exponentially and a linearly increasing component (see Fig. 3A, upper right). Following washout of ATP, the inward current deactivated with a fast and a slowly deactivating component as it has recently been described for the human receptor [18]. But usually, after washout of ATP, a slowly increasing conductance appeared (Fig. 3A, left). A further 4 s ATP pulse, after washout for 60 s, evoked again an inward

current of comparable amplitude, which added to the slowly increasing conductance. The slowly increasing conductance increased faster with further ATP applications. Upon final washout of the agonist, it deactivated within several minutes (indicated as dashed line in Fig. 3A, left and lower right; shown in Fig. 3B, left). In control measurements without application of ATP, we did not observe this increase in background current (not shown), showing that it is due to activation of $xP2X_7$. With BzATP as agonist, currents through $xP2X_7$ receptors showed the same behavior as currents activated by ATP (Fig. 3A, lower right). Apart from the slowly increasing conductance following washout of the agonist, this current behavior matches rather closely the behavior of human $P2X_7$ receptor expressed in oocytes [14,18]. In contrast, the rat subtype, when expressed in oocytes, undergoes a strong current run-down following activation [13].

The isoquinoline KN-62, a CAMK-II blocker, is an antagonist at the human and mouse $P2X_7$ receptor but has no effect on the rat subtype [19,6]. 1 μM of KN-62 is sufficient to completely inhibit activation of human $P2X_7$ receptors. Similar to the rat receptor, $xP2X_7$ was not inhibited by KN-62 (3 μM; Fig. 3B, left). A further property of $xP2X_7$, which is characteristic for $P2X_7$ receptors, was its block by extracellular divalent cations. 3 mM Mg^{2+} completely blocked the deactivating current as well as the slowly increasing conductance (Fig. 3B, middle trace). The approximate IC_{50} of 0.53 mM ($n = 4$–6, not shown) was similar to that reported for $rP2X_7$ (~0.47 mM; [20]). $P2X_7$ receptors are also inhibited by extracellular protons. At a pH, at which currents through the $rP2X_7$ receptor are half-maximally inhibited (~ pH 6.1; [20]), currents through the *Xenopus* subtype were already completely inhibited (Fig. 3B, right). Again, both the deactivating as well as the slowly increasing current component were inhibited. Inhibition of $xP2X_7$ was half-maximal at pH 7.7 ($n = 4$–7, not shown), meaning that $xP2X_7$ is significantly inhibited by extracellular protons under physiological conditions.

Determination of concentration–response curves with $P2X_7$ receptors is problematic. Current amplitude, evoked by equal agonist concentrations, was generally comparable but became more variable the larger the slowly increasing current component was. Therefore, we compared only two current amplitudes on the same oocyte, one evoked by the reference concentration of the agonist and the other evoked by a testing concentration of the agonist. EC_{50} was then calculated as described in Section 2. Due to these technical problems, EC_{50} values should be seen as estimates. Fig. 3C shows the normalized concentration–response curves for ATP and its analog BzATP: EC_{50} for ATP was approximately 2.6 mM ($n = 3$–5) and 139 μM for BzATP ($n = 2$–5). Thus, $xP2X_7$ is the least ATP-sensitive member of the P2X receptor family. Higher sensitivity to BzATP compared to ATP is a unique feature of $P2X_7$ receptors, clearly demonstrating that we indeed cloned the *X. laevis* homologue of the $P2X_7$ receptor. Altogether, $xP2X_7$ shows a unique combination of properties, known from human, mouse and rat $P2X_7$.

A slowly increasing current component has earlier been observed for $rP2X_7$ in *Xenopus* oocytes but was not accompanied by pore formation [13]. It has been reported that the large pore of $P2X_7$ receptors can be selectively blocked by HMA [21]. In Fig. 4A we demonstrate that the slowly increasing conductance, mediated by $xP2X_7$, could be completely blocked by HMA (100 μM). This represents a strong hint that $xP2X_7$ might be sufficient to induce formation of large pores in oocytes.

To analyze this property in more detail, we replaced Na^+ in the extracellular solution by $NMDG^+$. Under these conditions, ATP (1 mM) produced a slowly increasing inward current (Fig. 4B). Following washout of ATP, this inward current deactivated fast but only partially, followed by a slower, delayed deactivation process. To confirm formation of large pores, we applied repetitive voltage ramps from −120 mV to +20 mV within 1 s every 10 s. As is shown in Fig. 4C, the reversal potential significantly shifted to less negative values during activation of $xP2X_7$ receptors (from -59.0 ± 2.8 mV to -10.2 ± 3.6 mV within 5 min; $n = 8$; $P < 0.001$). This reflects an approximately seven-fold increase in relative permeability of $NMDG^+$ compared to Na^+ from 0.15 ± 0.02 to 1.01 ± 0.14 (Fig. 4D; $P < 0.001$). As a control, the same protocol was carried out with extracellular solution containing Na^+. During 5 min of ATP application the reversal potentials stayed stable (-10.2 ± 1.4 mV; $n = 8$; Fig. 4C, inset).

A further property of large pores, formed following activation of $P2X_7$ receptors, is the permeabilization of the plasma membrane for dye molecules such as the propidium dye YO-PRO-1. Incubation of $xP2X_7$ receptor expressing oocytes with extracellular solution containing BzATP (300 μM) and YO-PRO-1 (10 μM) for 5 min resulted in a fluorescence of whole oocytes indicating YO-PRO-1 uptake (Fig. 4E, left; $n = 6$; not quantified). In contrast, non-injected oocytes, which had been analyzed using this protocol, did not show any dye uptake (Fig. 4E, right; $n = 6$).

Block of the slowly increasing current component by HMA, increasing inward current caused by shift in reversal potential during prolonged $xP2X_7$ activation with $NMDG^+$ as extracellular cation, and YO-PRO-1 uptake clearly demonstrate pore formation. Thus, besides the unique pharmacological profile of $xP2X_7$, the most striking feature of this receptor is its ability to induce pore formation when expressed in *X. laevis* oocytes (consistent in oocytes from 14 different frogs). Therefore, the $xP2X_7$ receptor might prove a valuable tool to identify domains crucial for large pore formation.

Acknowledgements: We thank H.-S. Geisler for expert technical assistance. S.H. is student of the Tübingen Graduate School of Neural and Behavioural Sciences and is supported by a stipend of the Max-Planck-Gesellschaft. S.G. is supported by Grants of the Attempto research group program of the Universitätsklinikum Tübingen (FG 1-0-0) and the DFG (GR1771/3-1).

References

[1] Buell, G., Collo, G. and Rassendren, F. (1996) Eur. J. Neurosci. 8, 2221–2228.
[2] Newbolt, A., Stoop, R., Virginio, C., Surprenant, A., North, R.A., Buell, G. and Rassendren, F. (1998) J. Biol. Chem. 273, 15177–15182.
[3] Torres, G.E., Egan, T.M. and Voigt, M.M. (1998) FEBS Lett. 425, 19–23.
[4] Surprenant, A., Rassendren, F., Kawashima, E., North, R.A. and Buell, G. (1996) Science 272, 735–738.
[5] Rassendren, F., Buell, G.N., Virginio, C., Collo, G., North, R.A. and Surprenant, A. (1997) J. Biol. Chem. 272, 5482–5486.
[6] Chessell, I.P., Simon, J., Hibell, A.D., Michel, A.D., Barnard, E.A. and Humphrey, P.P. (1998) FEBS Lett. 439, 26–30.
[7] Cockcroft, S. and Gomperts, B.D. (1979) Nature 279, 541–542.
[8] Steinberg, T.H. and Silverstein, S.C. (1987) J. Biol. Chem. 262, 3118–3122.

[9] Di Virgilio, F. (1995) Immunol. Today 16, 524–528.
[10] Baricordi, O.R., Ferrari, D., Melchiorri, L., Chiozzi, P., Hanau, S., Chiari, E., Rubini, M. and Di Virgilio, F. (1996) Blood 87, 682–690.
[11] Gargett, C.E., Cornish, J.E. and Wiley, J.S. (1997) Br. J. Pharmacol. 122, 911–917.
[12] Khakh, B.S., Bao, X.R., Labarca, C. and Lester, H.A. (1999) Nat. Neurosci. 2, 322–330.
[13] Petrou, S., Ugur, M., Drummond, R.M., Singer, J.J. and Walsh Jr., J.V. (1997) FEBS Lett. 411, 339–345.
[14] Klapperstück, M., Büttner, C., Bohm, T., Schmalzing, G. and Markwardt, F. (2000) Biochim. Biophys. Acta 1467, 444–456.
[15] Madeja, M., Musshoff, U. and Speckmann, E.-J. (1995) J. Neurosci. Methods 63, 211–213.
[16] Zhang, Y., McBride Jr., D.W. and Hamill, O.P. (1998) J. Physiol. Lond. 508, 763–776.
[17] Deuchars, S.A. et al. (2001) J. Neurosci. 21, 7143–7152.
[18] Klapperstück, M., Büttner, C., Schmalzing, G. and Markwardt, F. (2001) J. Physiol. Lond. 534.1, 25–35.
[19] Humphreys, B.D., Virginio, C., Surprenant, A., Rice, J. and Dubyak, G.R. (1998) Mol. Pharmacol. 54, 22–32.
[20] Virginio, C., Church, D., North, R.A. and Surprenant, A. (1997) Neuropharmacology 36, 1285–1294.
[21] Nuttle, L.C. and Dubyak, G.R. (1994) J. Biol. Chem. 269, 13988–13996.